The International Journal of Advanced Manufacturing Technology (2019) 104:4605–4616
https://doi.org/10.1007/s00170-019-04316-7

ORIGINAL ARTICLE

A tunable passive damper for suppressing chatters in thin-wall milling by considering the varying modal parameters of the workpiece

Heng Yuan[1,2] · Min Wan[1,2] · Yun Yang[1,2] · Wei-Hong Zhang[1,2]

Received: 20 May 2019 / Accepted: 14 August 2019 / Published online: 29 August 2019

Abstract

Removal of the materials during thin-wall milling leads to obvious change of the modal parameters of the thin-walled workpiece. This article proposes a new method for designing a passive damper to suppress the chatters in thin-wall milling by considering the workpiece's in-process varying modal parameters. The modal parameters of the workpiece during cutting process is theoretically derived by including the influence of material removal, and the design principle of equal peaks is used to calculate the optimal parameters of the passive damper. Based on the derivation, the passive damper is then designed and manufactured. A series of milling experiments are conducted for the cases with and without the designed passive damper. Experimental observations show that the passive damper has good performance in suppressing chatters and improving the stability of the cutting system.

Keywords Milling · Chatter · Suppression · Passive damper

1 Introduction

Due to the advantages of large materials' removal rate and high efficiency and accuracy, milling is used as the most common processing technology to shape the thin-walled components widely used in the fields of aerospace and aviation [1]. Regenerative chatter, which is one of the most deleterious phenomena affecting machining operations and decreasing processing quality, is easy to occur during cutting process because of the weak stiffness of the workpiece [2, 3]. Many research efforts have been dedicated to the development of technologies that are able to predict and detect chatter to facilitate the avoidance of chatter during cutting process [4].

Accurate prediction of stability of lobe diagram (SLD), which provides the function between axial depth of cut and spindle speed, is an effective way to guide the selections of the cutting parameters to avoid the chatter. A lot of algorithms including zero-order method [1], semi-discretization method [5], full-discretization method [6], and multiple modes method [7] were proposed. Ren et al. [8] used the semi-discretization method to analyze the stability of thin-wall milling process and gave clearer insight into the dynamics and stability of thin-walled structure. Sun and Jiang [9] predicted chatter stability of the system by an extended second order semi-discretization method. Yan and Zhu [10] presented an improved multi-frequency solution to predict the critical axial dept of cut, and confirmed the good performance of the technique in chatter suppression. However, accurate stability lobe diagram just reflects the physical properties of the cutting system and avoids chatters by selecting proper cutting parameters.

To increase the stability of the cutting process, many techniques were also proposed [11–13]. Herranz et al. [14] proposed a working methodology for efficient process planning, which provides several steps that can minimize the bending and vibration effects. Mohring and Wiederkehr [15] presented intelligent fixtures for the mitigation of chatters in milling of thin-walled workpieces. Zhang et al. [16, 17] conducted a feasibility study by submerging the milling system in viscous fluid to mitigate milling chatter. Wan et al. [18] presented a stability improvement method in thin-wall milling by applying tensile prestress to the workpiece.

✉ Min Wan
m.wan@nwpu.edu.cn

1 School of Mechanical Engineering, Northwestern Polytechnical University, Xi'an, 710072, Shaanxi , China

2 State IJR Center of Aerospace Design and Additive Manufacturing, Northwestern Polytechnical University, Xi'an, 710072, Shaanxi, China

Besides the suppression strategies described above, there exists other methods focused on designing active or passive dampers to improve the stability of the cutting process [19]. Moradi et al. [20] designed a semi-active tunable vibration absorber to suppress regenerative chatter in milling process, and optimum values of the absorber are determined so that the cutting tool vibrations can be minimized. Zhang et al. [21] proposed a novel semi-active tuned mass damper, which is capable to extend its working frequency band through tuning the stiffness; however, no validation experiments were conducted.

Many efforts have been made to conduct further studies [22–24]. Zhang et al. [25] focused on the design of robust controller for chatter suppression, and experimental results show that the designed algorithm is able to suppress chatter. Wang et al. [26] proposed multi-harmonic stiffness excitation and random stiffness excitation method, and implemented milling experiments under stiffness excitation, which validated that the proposed method can suppress chatter effectively. Fei et al. [27] proposed a fixture element to enhance the stiffness of the workpiece in process so that the stability of the milling process could be improved. Yuan et al. [28] proposed a tunable mass damper to suppress the chatters when milling the cylindrical parts. Yang et al. [29, 30] suppressed chatters by designing tunable mass dampers and made good effects in improving the stability of the system.

It should be commented that although the researches mentioned above were devoted to developing effective methods to suppress chatters, they ignored the variety of the dynamic parameters of the workpiece due to the removal of materials. As reported in Refs. [31, 32], both natural frequency and mode shape vary greatly due to the reduction of the mass and the stiffness of the thin-walled workpiece. Thus, different from the existing studies, this paper designs a passive damper to suppress the chatters occurring in thin-wall milling by considering the variety of the dynamics of the workpiece due to the removal of materials. The design criteria considering the various dynamic parameters of the workpiece are described in Section 2. The structures of the passive damper are detailed in Section 3. In Section 4, a series of experiments are conducted with the designed passive damper, which show the good performance of the passive damper in improving machining stability. The article is concluded in Section 5.

2 Design principle considering varying stiffness of the workpiece

The dynamic governing equation of the workpiece to be machined at the initial status is expressed as follows.

$$\boldsymbol{M}_0\ddot{\boldsymbol{X}}(t) + \boldsymbol{C}_0\dot{\boldsymbol{X}}(t) + \boldsymbol{K}_0\boldsymbol{X}(t) = \boldsymbol{F}_0(t) \tag{1}$$

where $\boldsymbol{M}_0$, $\boldsymbol{C}_0$, and $\boldsymbol{K}_0$ denote the mass, damping, and stiffness matrices of the initial workpiece. $\boldsymbol{X}(t)$ is the displacement matrix of the workpiece. $\boldsymbol{F}_0(t)$ is the cutting force matrix acting on the initial workpiece. The relevant free vibration equation can be written as

$$\boldsymbol{M}_0\ddot{\boldsymbol{X}}(t) + \boldsymbol{K}_0\boldsymbol{X}(t) = 0 \tag{2}$$

The eigenvalue equation of Eq. 2 is expressed as follows.

$$\left(\boldsymbol{K}_0 - \omega_0{}^2\boldsymbol{M}_0\right)\boldsymbol{X}(\omega) = 0 \tag{3}$$

where ω_0 is natural frequency matrix of the initial workpiece. $\mathbf{X}(t)$ can be transformed from the physics space to the modal space by the following formula.

$$\boldsymbol{X}(t) = \boldsymbol{D}_0\boldsymbol{P}_0(t) \tag{4}$$

where $\boldsymbol{D}_0$ is the mass normalized modal shape matrix, which can be obtained by rearranging the eigenvectors related to the eigenvalue ω_0. $\boldsymbol{P}_0(t)$ is modal displacement matrix.

It should be mentioned that the dynamics of workpiece will be changed as the material of the workpiece is removed, and the dynamic governing equation of the workpiece during process can be expressed as follows.

$$\boldsymbol{M}_\mathrm{b}\ddot{\boldsymbol{X}}(t) + \boldsymbol{C}_\mathrm{b}\dot{\boldsymbol{X}}(t) + \boldsymbol{K}_\mathrm{b}\boldsymbol{X}(t) = \boldsymbol{F}_\mathrm{b}(t) \tag{5}$$

where $\boldsymbol{M}_\mathrm{b}$, $\boldsymbol{C}_\mathrm{b}$, and $\boldsymbol{K}_\mathrm{b}$ are the mass, damping, and stiffness matrices of the workpiece in process. $\boldsymbol{F}_\mathrm{b}(t)$ is the force matrix acting on the workpiece during process. The free vibration equation associated with Eq. 5 can be expressed as follows.

$$\boldsymbol{M}_\mathrm{b}\ddot{\boldsymbol{X}}(t) + \boldsymbol{K}_\mathrm{b}\boldsymbol{X}(t) = 0 \tag{6}$$

To solve the equation quickly, the mass matrix $\boldsymbol{M}_\mathrm{b}$ during process can be denoted as the sum of the initial mass matrix $\boldsymbol{M}_0$ and the removal mass matrix $\Delta\boldsymbol{M}$. The removal mass matrix $\Delta\boldsymbol{M}$ can be treated as a relatively small value by multiplying a softening coefficient. To reveal the influence of the removed material, the stiffness of the corresponding elements is treated as a relatively small value by multiplying a softening coefficient. The mass and stiffness during process can be expresses as

$$\begin{aligned}\boldsymbol{M}_\mathrm{b} &= \boldsymbol{M}_0 + \Delta\boldsymbol{M}\\ \boldsymbol{K}_\mathrm{b} &= \boldsymbol{K}_0 + \Delta\boldsymbol{K}\end{aligned} \tag{7}$$

By substituting Eq. 7 into Eqs. 6, 8 can be obtained as follows.

$$(\boldsymbol{M}_0 + \Delta\boldsymbol{M})\ddot{\boldsymbol{X}}(t) + (\boldsymbol{K}_0 + \Delta\boldsymbol{K})\boldsymbol{X}(t) = 0 \tag{8}$$

Substituting Eq. 4 into Eq. 8 and then multiplying $\boldsymbol{D}_0^\mathrm{T}$ to both sides of Eq. 8 give

$$\begin{aligned}&(\boldsymbol{D}_0^\mathrm{T}\boldsymbol{M}_0\boldsymbol{D}_0 + \boldsymbol{D}_0^\mathrm{T}\Delta\boldsymbol{M}\boldsymbol{D}_0)\ddot{\boldsymbol{P}}(t)\\ &+(\boldsymbol{D}_0^\mathrm{T}\boldsymbol{K}_0\boldsymbol{D}_0 + \boldsymbol{D}_0^\mathrm{T}\Delta\boldsymbol{K}\boldsymbol{D}_0)\boldsymbol{P}_0(t) = 0\end{aligned} \tag{9}$$

Because $\boldsymbol{D}_0$ is a mass normalized matrix, the following equations can be obtained.

$$\begin{aligned} \boldsymbol{D}_0^{\mathrm{T}} \boldsymbol{M}_0 \boldsymbol{D}_0 &= \boldsymbol{I} \\ \boldsymbol{D}_0^{\mathrm{T}} \boldsymbol{K}_0 \boldsymbol{D}_0 &= \omega_0^2 \end{aligned} \tag{10}$$

Substituting Eq. 10 into Eq. 9 leads to

$$(\boldsymbol{I} + \boldsymbol{D}_0^{\mathrm{T}} \boldsymbol{M}_0 \boldsymbol{D}_0) \ddot{\boldsymbol{P}}(t) + (\omega_0^2 + \boldsymbol{D}_0^{\mathrm{T}} \Delta \boldsymbol{K} \boldsymbol{D}_0) \boldsymbol{P}_0(t) = 0 \tag{11}$$

The eigenvalue equation of Eq. 11 can be denoted as follows.

$$\left[(\omega_0^2 + \boldsymbol{D}_0^{\mathrm{T}} \Delta \boldsymbol{K} \boldsymbol{D}_0) - \lambda (\boldsymbol{I} + \boldsymbol{D}_0^{\mathrm{T}} \boldsymbol{M}_0 \boldsymbol{D}_0) \right] \boldsymbol{P}_0(\omega) = 0 \tag{12}$$

where λ is the new eigenvalue of the workpiece during process. The relationship between $\boldsymbol{P}_0(t)$ and $\boldsymbol{P}_{\mathrm{b}}(t)$ can be obtained as follows.

$$\boldsymbol{P}_0(t) = \boldsymbol{D}_{\mathrm{r}} \boldsymbol{P}_{\mathrm{b}}(t) \tag{13}$$

where $\boldsymbol{D}_{\mathrm{r}}$ is the new transformation matrix related to the natural frequency of the workpiece. By substituting Eq. 13 into Eq. 4, the modal matrix during process $\boldsymbol{D}_{\mathrm{b}}$ can be obtained as follows.

$$\boldsymbol{D}_{\mathrm{b}} = \boldsymbol{D}_0 \boldsymbol{D}_{\mathrm{r}} \tag{14}$$

Then, the natural frequency ω_{b} of the workpiece during cutting process can be obtained from the new eigenvalue λ, and the mode shape m_{b} can be extracted from the modal matrix $\boldsymbol{D}_{\mathrm{b}}$.

The milling system with a passive damper is illustrated in Fig. 1. To effectively suppress the vibrations, the frequency ratio $\nu = \omega_{\mathrm{d}}/\omega_{\mathrm{b}}$ between the frequency of the passive damper ω_{d} and the frequency of the workpiece ω_{b} are introduced. The design criterion of equal peaks is used to calculate the optimal parameters of the passive damper, which is described as follows [33].

$$\nu = \frac{1}{1+\mu} \tag{15}$$

where μ is the mass ratio between the passive damper m_{d} and the targeted mode shape m_{b}. Finally, the optimal frequency of the passive damper can be calculated by

$$\omega_{\mathrm{d}} = \omega_{\mathrm{b}} \nu \tag{16}$$

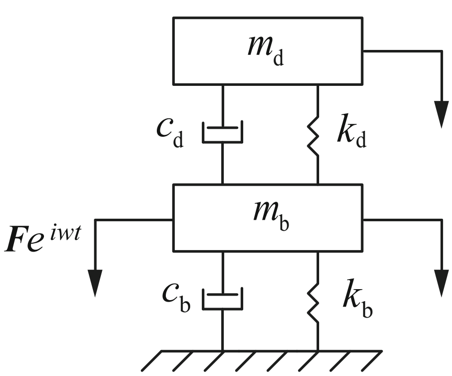

Fig. 1 Illustration of the system damped by a passive damper

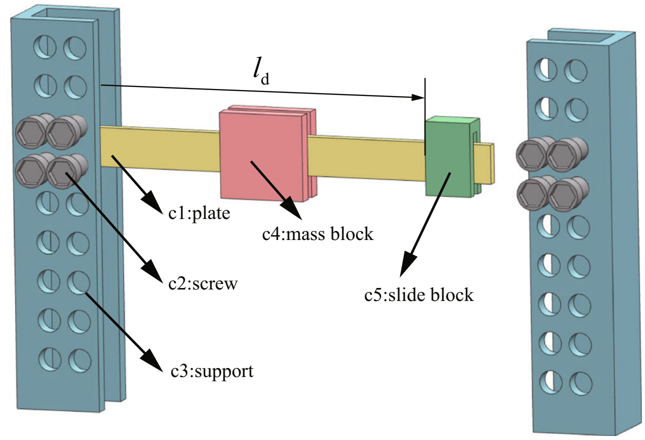

Fig. 2 Structures of the passive damper

3 Structures of the passive damper

To effectively reduce the vibrations, the passive damper with tunable stiffness is designed according to the principle described in Section 2. The structure of the passive damper is illustrated in Fig. 2. The passive damper mainly consists of five components. c1 is the thin plate. c4 is the mass block, which is fixed on the middle part of the thin plate (c1). The slide blocks (c5) at both sides of c4 can slide along the thin plate, and this characteristic means that the length between the two fixed points can be adjusted. The frequency of the passive damper is adjustable through changing the length of the thin plate. The screws (c2) are used to fix the slide blocks (c5). c3 is the component, which gives a support for the damper. The thin plate (c4) can be moved up and down along the support (c3).

To clearly describe the relationship between the frequency of the passive damper and the length of the thin

Table 1 The frequency of the passive damper under different length (l_{d})

l_{d} (mm)	42	43	44	45	46	47	48	49	50	51	52	53	54
ω_{d} (Hz)	774	739	708	678	650	625	601	578	557	537	519	500	484

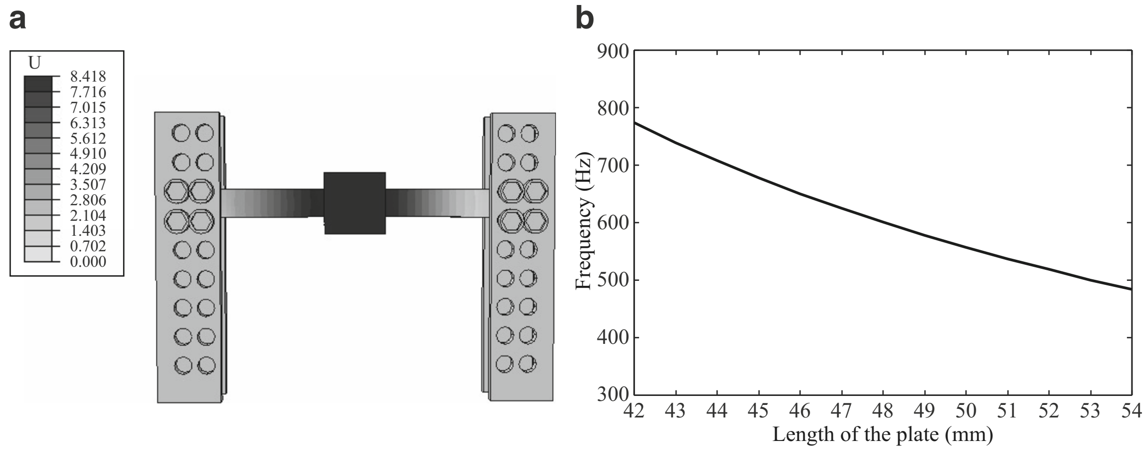

Fig. 3 Results of modal analysis of the passive damper

plate, modal analysis of the passive damper is completed though finite element method. The results of modal analysis are listed in Table 1 and plotted in Fig. 3.

To further show how to suppress the vibrations through the passive damper, the procedure of conduction is summarized as follows.

1. Choose the workpiece and obtain the modal parameters of the initial workpiece by finite element method.
2. Calculate the dynamic modal parameters of the workpiece in process and extract the natural frequency ω_b and mode shape m_b from the modal parameters by using the method described in Section 2.
3. Design the passive damper, which is schematically shown in Fig. 2, according to the modal parameters of the workpiece.
4. Establish the relationship between the natural frequency ω_d and the adjustable length l_d of the passive damper.
5. Calculate the mass ratio μ and optimal frequency ω_d of the passive damper by using the design principle expressed in Section 2.
6. Adjust the passive damper to the optimal position according to the results of steps (4) and (5).

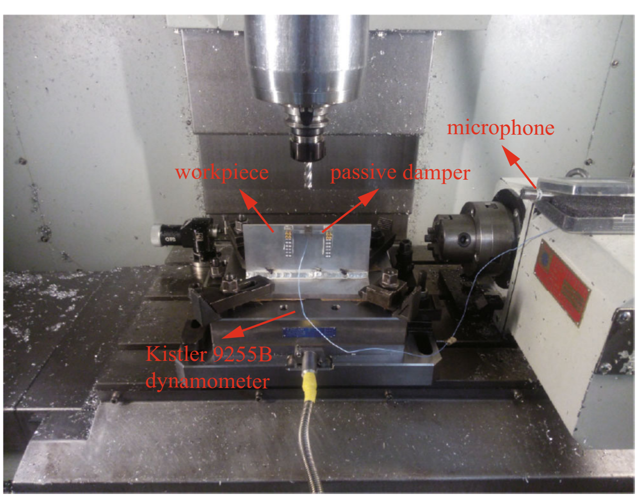

Fig. 4 Experimental setup

4 Experimental verification

To verify the effectiveness of the proposed method, a series of tests have been conducted on a three-axis CNC machining center. A four-fluted carbide tool with the diameter being 12 mm is used. In the experiments, a microphone is used to acquire the sound signals. Kistler 9255B dynamometer is used to measure the force signals. The experimental setup is illustrated in Fig. 4.

The workpiece with the material being aluminum alloy AL 7075 and the size being 180 mm $\times$ 80 mm $\times$ 5 mm is used. It should be pointed out that the workpiece used in the experiments is a thin-walled plate, which has much higher stiffness in X-direction than that in Y-direction. Therefore, the passive damper is mainly designed to focus on the vibrations in Y-direction. Because of this understanding, the illustration of the system damped by the passive damper

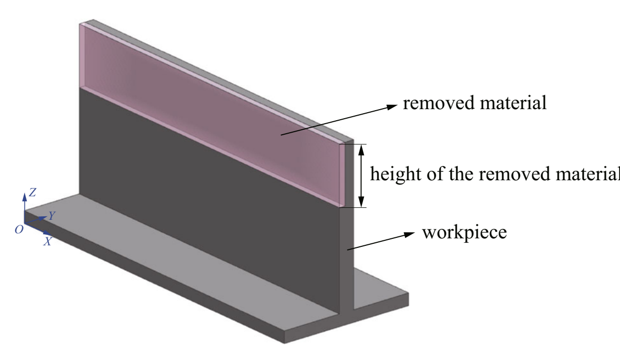

Fig. 5 Illustration of the removed materials

Table 2 Calculation results of the dynamics of the workpiece in process

Height of the material removal (mm)	Frequency ω_b (Hz)	Normalized mass ($1/\sqrt{kg}$)
0	645.4	4.2954
2.5	661.4	4.1996
5.0	677.1	4.0927
7.5	692.3	3.9809
10.0	707.0	3.8547
12.5	721.0	3.7190
15.0	734.1	3.5737
17.5	746.0	3.4139
20.0	756.5	3.2393
22.5	765.1	3.0514
25.0	771.5	2.8479
27.5	775.1	2.6298
30.0	775.7	2.3973
32.5	772.5	2.1547
35.0	765.6	1.9059
37.5	754.5	1.6568
40.0	739.9	1.4139

Table 3 Calculation results of the optimal frequency of the passive damper

Height of the material removal (mm)	Mass ratio μ	Frequency ratio ν	Optimal frequency ω_d (Hz)
0	0.2528	0.7982	515.2
2.5	0.2416	0.8054	532.7
5.0	0.2295	0.8133	550.7
7.5	0.2171	0.8216	568.8
10.0	0.2036	0.8308	587.4
12.5	0.1895	0.8407	606.1
15.0	0.1750	0.8511	624.8
17.5	0.1597	0.8623	643.3
20.0	0.1438	0.8743	661.4
22.5	0.1276	0.8868	678.5
25.0	0.1111	0.9000	694.4
27.5	0.0947	0.9135	708.1
30.0	0.0787	0.9270	719.1
32.5	0.0636	0.9402	726.3
35.0	0.0498	0.9526	729.3
37.5	0.0376	0.9638	727.2
40.0	0.0274	0.9733	720.1

is only shown to have one degree of freedom in Fig. 1. The radial depth of cut is 2 mm. As the cutting continues, the removal of the materials will be increased, as shown in Fig. 5. The dynamic properties of the workpiece will be changed with the removal of the materials. It is worth noting here that the mode shape plays a significant role on the FRF, and the FRFs change at different cutting points. Thus, in the experiments, after the current tool path of cutting is completed, new mode shape of the specified point in the next tool path is updated by using the method described in Section 2. The natural frequency and normalized mass of the point, which will be cut in the next tool path, are calculated by considering the removal of the materials. The results are listed in Table 2 and plotted in Fig. 6.

The passive damper is attached to the workpiece' s opposite side of the surface to be machined by Blu. Tack glue. To comprehensively balance the influences of the left and right parts of the workpiece, the passive damper is located at the middle position of the thin-walled plate along the feed direction. Besides, since the upper part of the workpiece has weaker stiffness than the lower part along the height direction, the passive damper should be tried to fix on the relatively higher part of the workpiece. Finally, it should be mentioned that quantitative study of the influence of the location of the passive damper is not the key issue to be studied here, and it remains as a further problem to be deeply detected. The mass of the passive damper is 13.7 g.

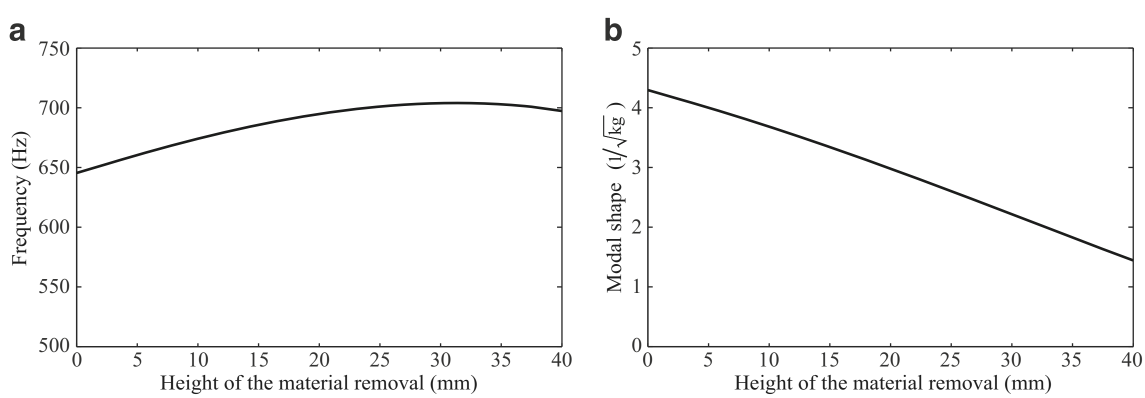

Fig. 6 Dynamics of the workpiece in process. **a** Natural frequency of the workpiece. **b** Normalized mass

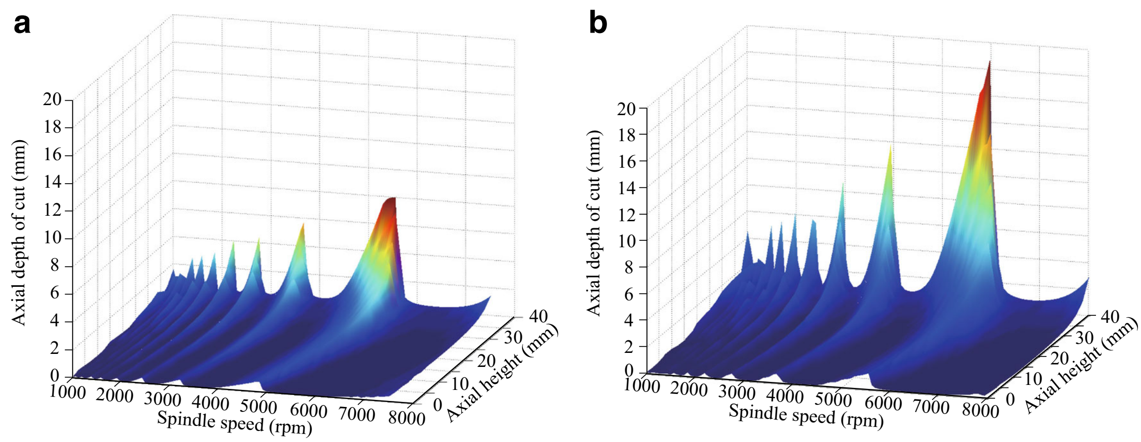

Fig. 7 Stability lobe diagrams without and with passive damper. **a** Without passive damper. **b** With passive damper

Fig. 8 Experimental results at spindle speed of 3500 rpm when the height of the material removal is zero. "SF" denotes integer times of tooth passing frequency. "CF" denotes chatter frequency. "TMD" denotes tunable mass damper

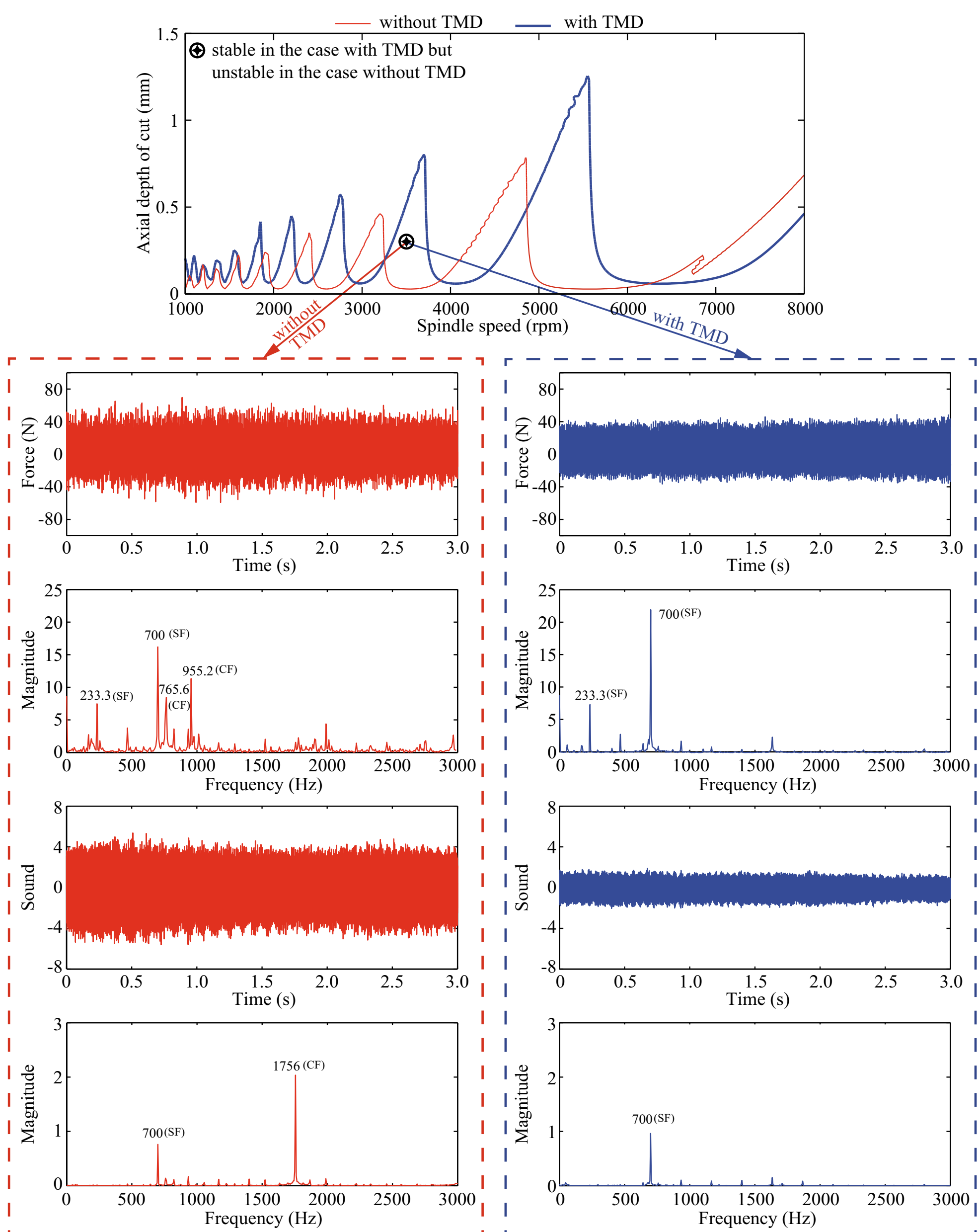

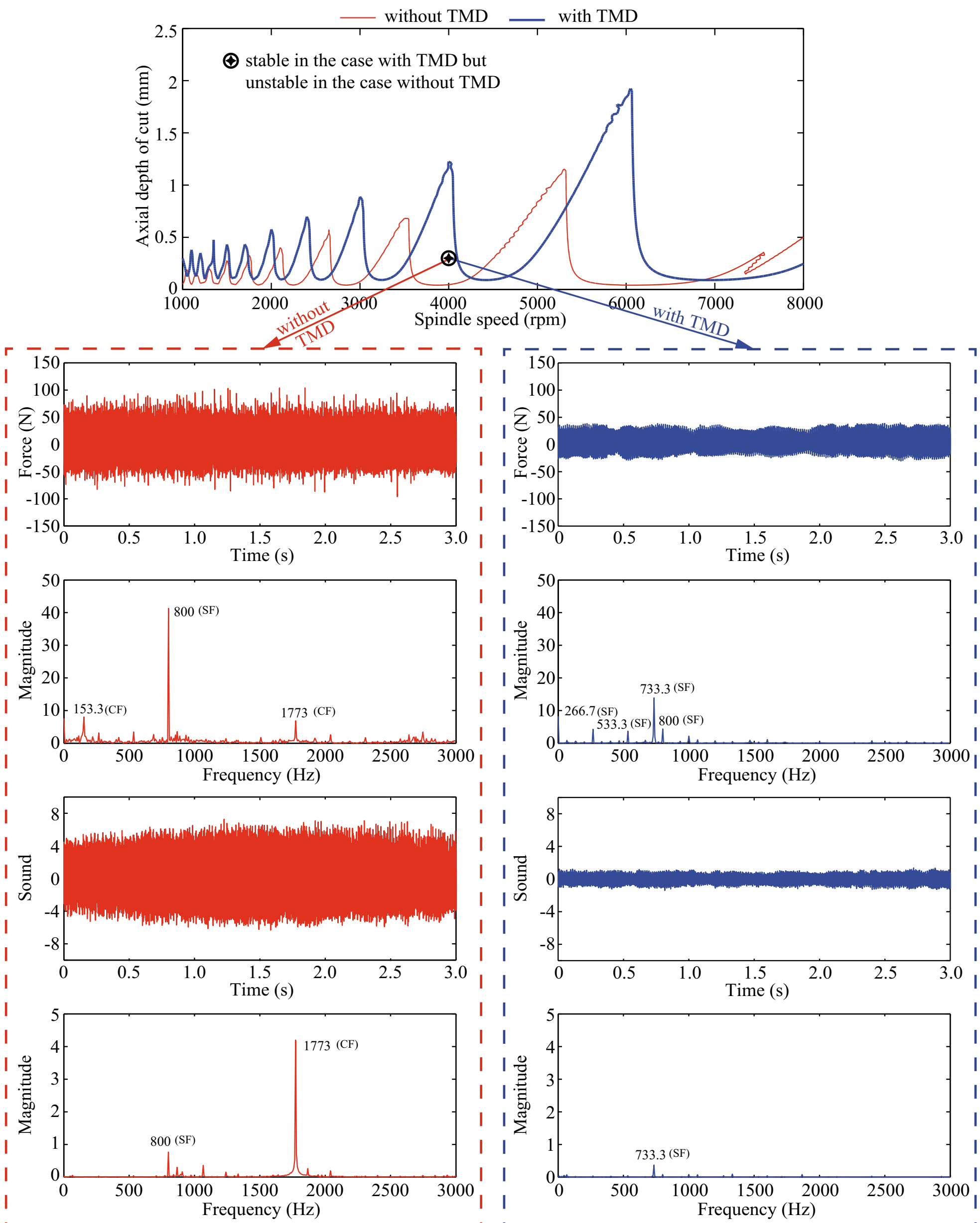

Fig. 9 Experimental results at spindle speed of 4000 rpm when the height of the material removal is 10 mm. "SF" denotes integer times of tooth passing frequency. "CF" denotes chatter frequency. "TMD" denotes tunable mass damper

The mass ratio and optimal frequency of the passive damper are calculated, and the results are listed in Table 3.

Finally, the following comments should be concerned. In actual milling process, the passive damper does not need to be adjusted along a certain tool path. But, after a tool path is completed, the new mode shape of the specified point in the next tool path should be calculated by using the method described in Section 2. Then, the optimal frequency of the passive damper is obtained as Eqs. 15 and 16. The length l_d shown in Fig. 2 can be determined according to the relationships between the frequency of the passive damper and the length l_d, as shown in Table 1. That is, l_d can be tuned by adjusting the two slide blocks (c5) along the plate (c1) to its calculated length. Finally, the thin plate (c1) and two slide blocks (c5) together with the mass block (c4) are adjusted along the supports (c3) to make sure the mass block (c4) is at the opposite side of the specified cutting point in the next tool path to be suppressed. The whole operations are manually carried out.

To show the performance of the passive damper, the 3D stability lobe diagrams without and with passive damper are plotted in Fig. 7. It can be seen that axial critical depths of cut increase obviously when the passive damper works. To further validate the effectiveness of the passive damper, the experiments at three different positions, corresponding to which different ratios of materials are removed, are conducted.

It should be mentioned that in the milling process of the cantilevered thin-walled workpiece, the bending mode is the most significant factor that influences the vibrations of the workpiece. Because of this fact, this article aims to design a passive damper for the suppression of the workpiece' s first order of bending mode. Anyway, the second or other modes also influence the stability of the cutting process, and how to include the influence of these models remains as an open problem to be further studied.

When the height of the material removal is zero, the experiment is conducted at the spindle speed of 3500 rpm. The feed rate is 0.05 mm/tooth. The radial depth of cut is 2 mm. The axial depth of cut is 0.3 mm. The tooth passing frequency is 58.33 Hz. The sound signals and force signals together with their Fourier transformation with and without passive damper are shown in Fig. 8. From the figure, it can be seen that when there is no passive damper, 765.6 Hz and 955.2 Hz occur in the sound signals and 1756 Hz occurs in the force signals, and these frequencies are not integral times of the tooth passing frequency. That means chatters occur during the cutting process and the system is not stable. While the dominant frequency occurs in the sound and force signals are all integral times of the tooth passing frequency when the passive damper is applied to the system.

Another group of experiment is conducted when the height of the material removal is 10 mm. In this experiment, the spindle speed is 4000 rpm. The feed rate is 0.05 mm/tooth. The radial depth of cut is 2 mm. The axial depth of cut is 0.3 mm. The tooth passing frequency is 66.67 Hz. The experimental results of sound and force signals together with their

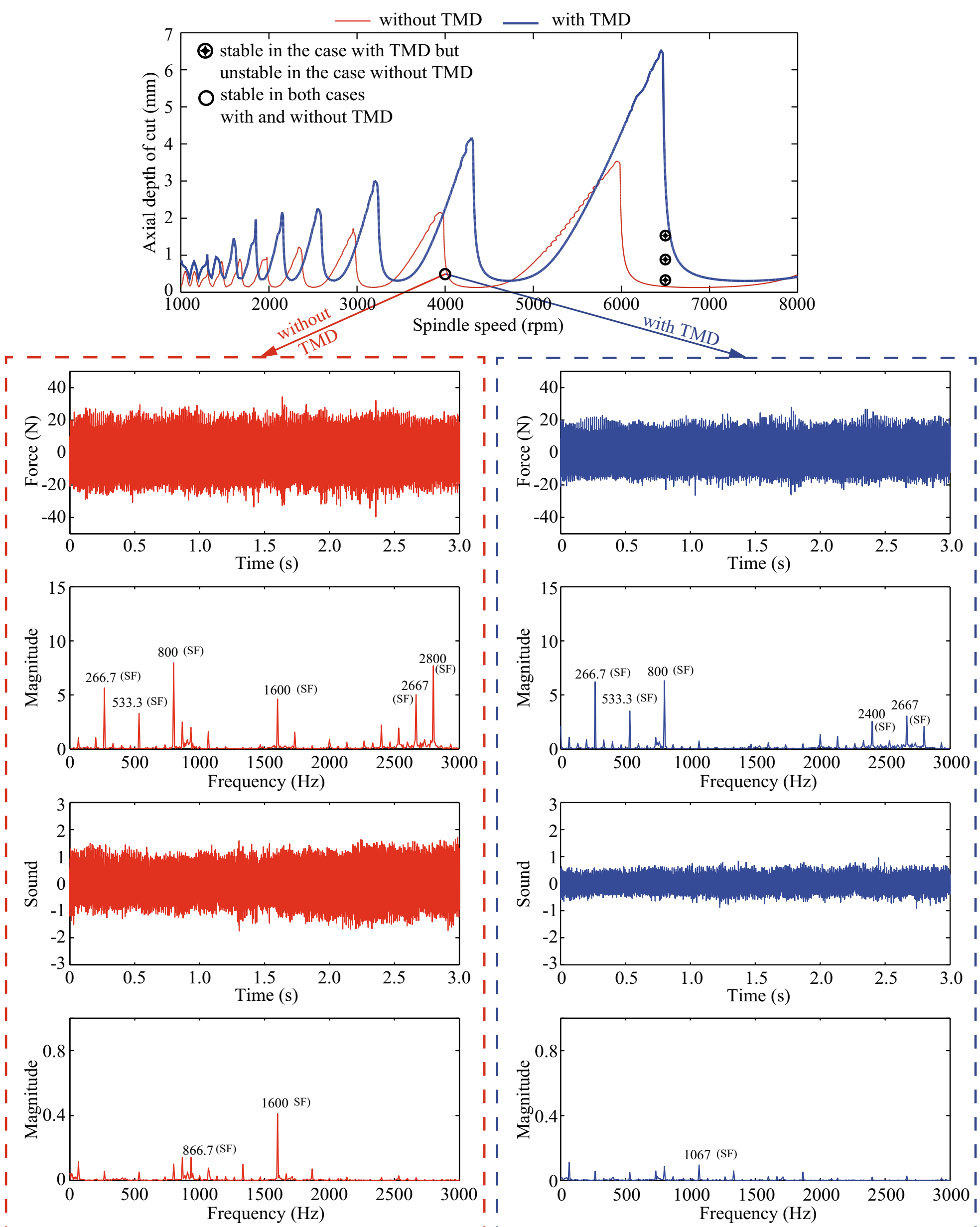

Fig. 10 Experimental results at spindle speed of 4000 rpm when the height of the material removal is 30 mm. "SF" denotes integer times of tooth passing frequency. "CF" denotes chatter frequency. "TMD" denotes tunable mass damper

Fourier transformation are illustrated in Fig. 9. From the collected signals in Fig. 9, it can be clearly seen that the chatter frequency of 1773 Hz occurred both in sound signals, and force signals are not integral multiples of the tooth passing frequency. That is, the system is not stable when the passive damper is off. Besides, the magnitudes of the sound and force signals without passive damper are much bigger than that with passive damper. This phenomenon shows the good performance of the passive damper.

When the height of the material removal is 30 mm, the experiment is conducted at the spindle speed of 4000 rpm. The feed rate is 0.05 mm/tooth. The radial depth of cut is 2 mm. The axial depth of cut is 0.5 mm. The tooth passing frequency is 66.67 Hz. The experimental results are shown in Fig. 10. According to the collected sound and force signals together with their Fourier transformation, it can be seen that the frequencies occurring in the Fourier transformation are all integer multiples of the tooth passing frequency whether the system is with or without the passive damper. This means that there are no chatters during the cutting process under the two conditions. However, from the figure, it can be seen that when the passive damper is on, the magnitudes of the sound and force signals decrease obviously than that without the passive damper. This phenomenon implies the good performance of the passive damper in reducing vibrations.

Another experiment at the height of the material removal of 30 mm is conducted under the cutting condition of

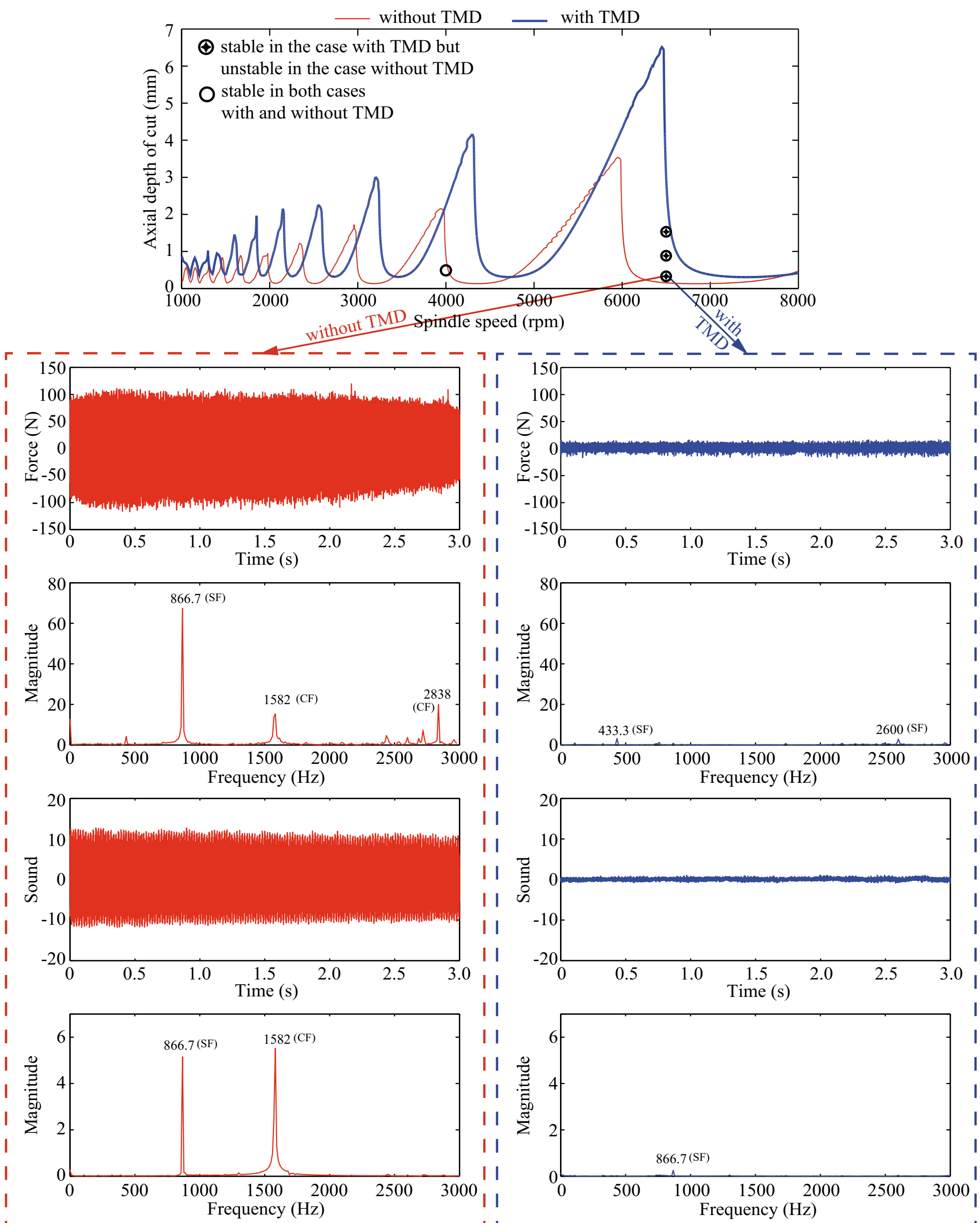

Fig. 11 Experimental results at spindle speed of 6500 rpm when the height of the material removal is 30 mm. “SF” denotes integer times of tooth passing frequency. “CF” denotes chatter frequency. “TMD” denotes tunable mass damper

spindle speed of 6500 rpm. The feed rate is 0.05 mm/tooth. The radial depth of cut is 2 mm. The axial depth of cut is 0.3 mm. The tooth passing frequency is 108.33 Hz. The collected sound and force signals and their Fourier transformation are illustrated in Fig. 11. It can be obviously seen that chatter occurs at the frequency of 1582 Hz both in sound signals and force signals when the system is without the passive damper, while the cutting process is stable when the passive damper is used in the cutting system. What's more, compared with the sound and force signals without the passive damper, the magnitudes of the sound and force signals are much more smaller. Other two groups of experiments are also conducted at spindle speed of 6500 rpm. The axial depths of cut are increased to 0.8 mm and 1.5 mm when the passive damper is used. The experimental results of these two conditions are shown in Fig. 12. From the Fourier transformations of sound and force signals, it can be seen that the cutting system remains stable though the axial depth of cut is up to 1.5 mm when the passive damper is on. It shows good performance of the passive damper.

According to the experiments conducted and stability analysis of the collected sound and force signals together with their Fourier transformation above, it can be obviously seen that the magnitudes of the measured signals are more smaller and no chatter occurs when the designed passive damper is attached to the cutting system. These phenomenon shows the good performance of the designed passive damper in improving the stability of cutting system.

Fig. 12 Experimental results at spindle speed of 6500 rpm when the height of the material removal is 30 mm. "SF" denotes integer times of tooth passing frequency. "TMD" denotes tunable mass damper

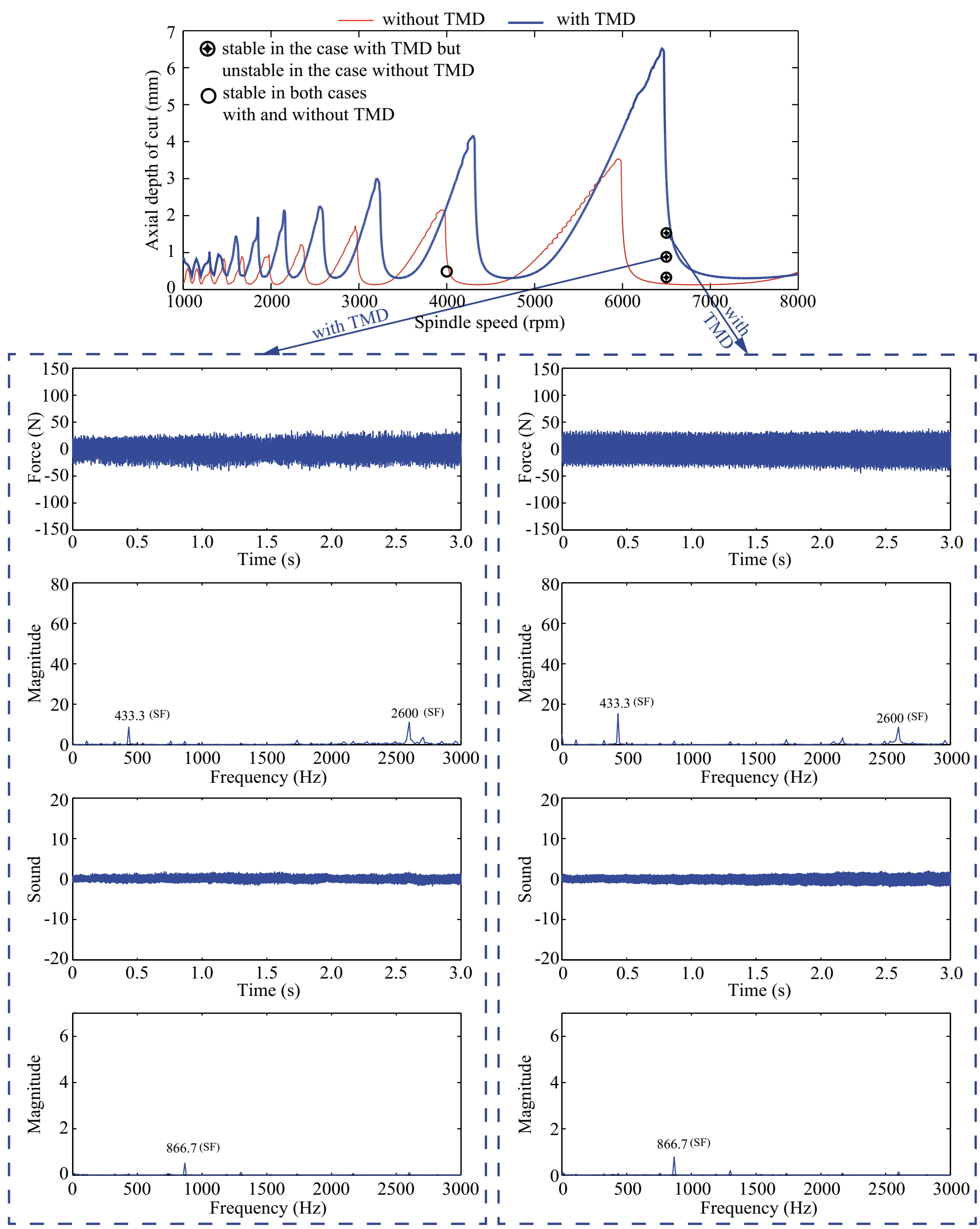

5 Conclusions

Chatters are easy to occur in the milling process of thin-walled components, and thus constitute a harmful source to stable machining. To suppress the vibrations and improve the stability of the cutting system, a passive damper is designed and manufactured with tunable stiffness. The modal parameters of the workpiece during cutting process are derived and the design criterion of equal peaks is used to calculate the optimal frequency of the passive damper. To validate the effectiveness of the proposed method and designed passive damper, a series of experiments are conducted with and without passive damper. During the experiments, the sound signals and force signals are measured and their Fourier transformation are calculated. The results of the experiments show that the cutting system are more stable when the passive damper is used, and it proves the good performance of the passive damper in suppressing chatters and improving the stability of the system.

Funding information This research has been supported by the National Natural Science Foundation of China under Grant no. 51675440, National Key Research and Development Program of China under Grant no. 2017YFB1102800, and the Fundamental Research Funds for the Central Universities under Grant no. 3102018gxc025.

References

1. Altintas Y (2012) Manufacturing automation, 2nd ed. Cambridge University
2. Albertelli P, Braghieri L, Torta M, Monno M (2019) Development of a generalized chatter detection methodology for variable speed machining. Mech Syst Signal Process 123:26–42
3. Cen LJ, Melkote SN, Castle J, Appelman H (2018) A method for mode coupling chatter detection and suppression in robotic milling. Trans ASME J Manuf Sci Eng 140:081015
4. Yue CX, Gao HN, Liu XL, Steven YL, Wang LH (2019) A review of chatter vibration research in milling. Chin J Aeronaut 32(2):215–242
5. Insperger T, Stepan G (2004) Updated semi-discretization method for periodic delay-differential equations with discrete delay. Int J Numer Methods Eng 61:117–141
6. Ding Y, Zhu LM, Zhang XJ, Ding H (2010) A full-discretization method for prediction of milling stability. Int J Mach Tools Manuf 50:502–509
7. Wan M, Ma YC, Zhang WH, Yang Y (2015) Study on the construction mechanism of stability lobes in milling process with multiple modes. Int J Adv Manuf Technol 79:589–603
8. Ren S, Long XH, Meng G (2018) Dynamics and stability of milling thin walled pocket structure. J Sound Vib 429:325–347
9. Sun YW, Jiang SL (2018) Predictive modeling of chatter stability considering force-induced deformation effect in milling thin-walled parts. Int J Mach Tools Manuf 135:38–52
10. Yan BL, Zhu LD (2019) Research on milling stability of thin-walled parts based on improved multi-frequency solution. Int J Adv Manuf Technol 102:431–441
11. Munoa J, Beudaert X, Dombovari Z, Altintas Y, Budak E, Brecher C, Stepan G (2016) Chatter suppression techniques in metal cutting. CIRP Ann-Manuf Technol 65:785–808
12. Zhang XM, Zhang D, Cao L, Huang T, Leopold J, Ding H (2017) Minimax optimization strategy for process parameters planning: toward interference-free between tool and flexible workpiece in milling process. Trans ASME J Manuf Sci Eng 139:051010
13. Feng J, Wan M, Gao TQ, Zhang WH (2018) Mechanism of process damping in milling of thin-walled workpiece. Int J Mach Tools Manuf 134:1–19
14. Herranz S, Campa FJ, Lopez De Lacalle LN, Rivero A, Lamikiz A, Ukar E, Sanchez J, Bravo U (2005) The milling of airframe components with low rigidity: a general approach to avoid static and dynamic problems. Proc Institut Mech Eng Part B: J Eng Manuf 219:789–801
15. Mohring HC, Wiederkehr P (2016) Intelligent fixtures for high performance machining. Procedia CIRP 46:383–390
16. Zhang Z, Li HG, Meng G, Ren S (2017) Milling chatter suppression in viscous fluid: a feasibility study. Int J Mach Tools Manuf 120:20–26
17. Zhang Z, Li HG, Liu XB, Zhang WY, Meng G (2018) Chatter mitigation for the milling of thin-walled workpiece. Int J Mech Sci 138-139:262–271
18. Wan M, Gao TQ, Feng J, Zhang WH (2019) On improving chatter stability of thin-wall milling by prestressing. J Mater Process Technol 264:32–44
19. Moradi H, Vossoughi G, Movahhedy MR, Salarieh H (2013) Suppression of nonlinear regenerative chatter in milling process via robust optimal control. J Process Control 23:631–648
20. Moradi H, Bakhtiari Nejad F, Movahhedy MR, Vossoughi G (2012) Stability improvement and regenerative chatter suppression in nonlinear milling process via tunable vibration absorber. J Sound Vib 331:4668–4690
21. Zhang L, Hong L, Dhupia JS, Johnson S, Qaiser Z, Zhou ZD (2018) A novel semi-active tuned mass damper with tunable stiffness. In: 2018 IEEE/ASME international conference on advanced intelligent mechatronics (AIM), pp 274–279
22. Zaeh M, Kleinwort R, Fagerer P, Altintas Y (2017) Automatic tuning of active vibration control systems using inertial actuators. CIRP Ann-Manuf Technol 66:365–368
23. Chen F, Zhao H (2018) Design of eddy current dampers for vibration suppression in robotic milling. Adv Mech Eng 10(11):1–15
24. Yao Q, Luo M, Zhang DH, Wu BH (2018) Identification of cutting force coefficients in machining process considering cutter vibration. Mech Syst Signal Process 103:39–59
25. Zhang XW, Wang CX, Liu JX, Yan RQ, Cao HR, Chen XF (2019) Robust active control based milling chatter suppression with perturbation model via piezoelectric stack actuators. Mech Syst Signal Process 120:808–835
26. Wang CX, Zhang XW, Liu JX, Yan RQ, Cao HR, Chen XF (2019) Multi harmonic and random stiffness excitation for milling chatter suppression. Mech Syst Signal Process 120:777–792
27. Fei JX, Lin B, Xiao JL, Ding M, Yan S, Zhang XF, Zhang J (2018) Investigation of moving fixture on deformation suppression during milling process of thin-walled structures. J Manuf Process 32:403–411
28. Yuan H, Wan M, Yang Y (2019) Design of a tunable mass damper for mitigating vibrations in milling of cylindrical parts. Chin J Aeronaut 32(3):748–758
29. Yang YQ, Dai W, Liu Q (2015) Design and implementation of two-degree-of-freedom tuned mass damper in milling vibration mitigation. J Sound Vib 335:78–88
30. Yang YQ, Xie RC, Liu Q (2017) Design of a passive damper with tunable stiffness and its application in thin-walled part milling. Int J Adv Manuf Technol 89:2713–2720
31. Yang Y, Zhang WH, Ma YC, Wan M (2016) Chatter prediction for the peripheral milling of thin-walled workpieces with curved surfaces. Int J Mach Tools Manuf 109:36–48

32. Yang Y, Zhang WH, Ma YC, Wan M, Dang XB (2019) An efficient decomposition-condensation method for chatter prediction in milling large-scale thin-walled structures. Mech Syst Signal Process 121:58–76
33. Den Hartog JP (1985) Mechanical vibrations. Courier Corporation